Radiation-Laminar Free Convection in a Square Duct with Specular Reflection by Absorbing-Emitting Medium

Ki-Hong Byun*

Department of Mechanical Engineering, Dongguk University, Seoul 100-715, Korea

Moon Hyuk Im

Department of Automotive and Mechanical Engineering, Keimyung University,
Daegu 704-701, Korea

The purpose of this work is to study the effects of specularly reflecting wall under the combined radiative and laminar free convective heat transfer in an infinite square duct. An absorbing and emitting gray medium is enclosed by the opaque and diffusely emitting walls. The walls may reflect diffusely or specularly. Boussinesq approximation is used for the buoyancy term. The radiative heat transfer is evaluated using the direct discrete ordinates method. The parameters under considerations are Rayleigh number, conduction to radiation parameter, optical thickness, wall emissivity and reflection mode. The differences caused by the reflection mode on the stream line, and temperature distribution and wall heat fluxes are studied. Some differences are observed for the categories mentioned above if the order of the conduction to radiation parameter is less than order of 10^{-3} for the range of Rayleigh number studied. The differences at the side wall heat flux distributions are observed as long as the medium is optically thin. As the top wall emissivity decreases, the differences between these two modes are increased. As the optical thickness decreases at the fixed wall emissivity, the differences also increase. The difference of the streamlines or the temperature contours is not as distinct as the side wall heat flux distributions. The specular reflection may alter the fluid motion.

Key Words : Specular, Diffuse Reflection, Radiation, Free Convection, Participating Media, Square Duct, Direct Discrete Ordinates Method

Nomenclature

c_k : k-direction cosines
I : Intensity, W/m^2-sr
L : Length of system, m
M_0 : Number of ordinates in one quadrant
n : Number of spatial divisions
N : $k/(4L\sigma T_r^3)$, conduction to radiation parameter
Pr : ν/α (kinematic viscosity/thermal diffusivity), Prandtl Number
Q : Dimensionless wall heat flux

$Q = q_{w}/(\sigma T_r^4)$
Ra : $g\beta(T_s-T_0)L^3/(\nu\alpha)$, Rayleigh number
T_0 : Reference temperature for fluid property, K
T_r : Reference temperature for radiation, K

Greeks

α : Thermal diffusivity
β : Volumetric thermal expansion coefficient, K^{-1}
ε : Wall emissivity
κ : Absorption coefficient, m^{-1}
ν : Kinematic viscosity
ρ : $1-\varepsilon$, reflectivity
σ : Stefan-Boltzmann coefficient, $W/m^2 \cdot K^4$
τ : κL, optical thickness
ω_k : k-discrete ordinate weighting factor
ξ_k, μ_k : y-direction, x-direction cosine

* Corresponding Author,
  E-mail : khbyun@dongguk.edu
  TEL : +82-2-2260-3701; FAX : +82-2-2263-9379
  Department of Mechanical Engineering, Dongguk University, Jung-Ku, Seoul 100-715, Korea. (Manuscript Received March 11, 2002; Revised July 5, 2002)

Subscripts

k : k-discrete ordinate direction

N, S, E, W : North, south, east, west

wall : Wall, $wall = N, S, E, W$

1. Introduction

The combined heat transfer of radiation and natural convection occurs in many engineering applications, such as HVAC, solar energy systems, fins, and room fire. Therefore, many previous investigations and reports are available in the literature. Lauriat (1982) studied the thermal radiation with laminar natural convection using P-1 approximation. A gray fluid in a rectangular cavity with aspect ratio of 5 to 20 is considered. The cavity has two isothermal side walls and two adiabatic end walls. The ranges of values of his study are Ra upto 10^6, N from 0.2 to 1, τ from 1 to 2, wall emissivity from 0 to 1. He concluded that radiation attenuates the intensity of the flow at low Rayleigh numbers and, in contrast, leads to an increase in flow strength in convection regimes. Tan and Howell (1991) studied the same system under consideration using the product–integral method and finite difference method. The range of Ra studied is 10^3, 10^4, 10^5, when N is varied from 0 to infinity. Fusegi and Farouk (1988) studied numerically and experimentally the interaction of laminar/turbulent natural convection in a square cavity filled with a non-gray gas. They used the P-1 approximation and the weighted sum of gray gases model for the non-gray gas. The radiation strongly alters the flow and temperature fields within a differentially heated square cavity. Heat transfer to the isothermal walls is greatly enhanced by radiation.

Iwatsu and Hyun (1996) studied the natural convection within a square enclosure with large temperature differences. They show the discrepancies between the idealized Boussinesq fluid model and the actual compressible fluid model of their laboratory experiments. Lee and Lee (1988) studied the natural convection in a 3-D rectangular enclosure. The results show that the temperature disturbances imposed on the end wall reinforces the axial flow and magnifies the three

dimensional effects. Bae, Jung, and Jeong (2002) studied the effects of partitions in ventilated square duct by numerically and experimentally. The laminar free convective heat transfer is considered, but the effect of the radiative heat transfer was not studied. The effects of the number and length of the partitions on the heat transfer characteristics are studied.

Sanchez and Smith (1992) investigated radiative heat transfer for a two dimensional rectangular system enclosing a transparent medium using the discrete-ordinates method (DOM) (Fiveland, 1984). Byun and Smith (1997a, b, 1998, 2001) reported that the view factors, the direct exchanger areas (DEA), and the total exchange areas (TEA) can be calculated accurately by using the direct discrete-ordinates method (DS_N).

Maruyama (1993) presented a numerical method for predicting radiative heat transfer between arbitrary three-dimensional bodies with specular and diffuse surfaces. The view factors were computed by using the ray tracing method. Cai (1998) presented a radiative heat transfer model for arbitrary multidimensional geometry enclosing a transparent or emitting, absorbing and isotropically scattering media with diffuse or specular walls. The ray-tracing technique was used and the generalized exchange factors were defined without using a matrix operation.

The purpose of this work is to study the effect of specularly reflecting walls on combined radiative and laminar free convective heat transfer in an infinite square duct. The parameters under considerations are Rayleigh number, conduction to radiation parameter, optical thickness, wall emissivity and reflection mode.

Another objective is to show that the direct discrete ordinate method can be applied to solve the problem with specularly reflecting walls.

2. Analysis

2.1 Governing equations

The system under study is an infinite square duct as depicted in Fig. 1 with the coordinate system. Some of the walls are diffusely emitting but reflecting diffusely or specularly. The medium
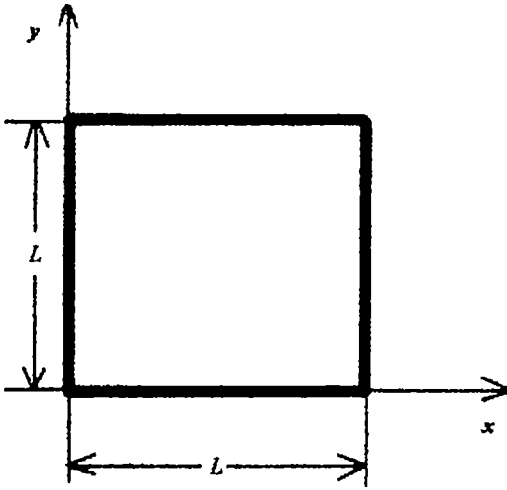
Fig. 1 System description

in the system is gray, absorbing and emitting, uniform, and in local thermodynamic equilibrium. It is assumed that laminar natural convective and thermal radiative heat transfer occur simultaneously. The width of the square duct is L.

The governing equations are as follows :

$$\frac{\partial u}{\partial x}+\frac{\partial v}{\partial y}=0 \tag{1}$$

$$\rho\left(u\frac{\partial u}{\partial x}+v\frac{\partial u}{\partial y}\right)=-\frac{\partial p}{\partial x}+\mu\left(\frac{\partial^2 u}{\partial x^2}+\frac{\partial^2 u}{\partial y^2}\right) \tag{2}$$

$$\rho\left(u\frac{\partial v}{\partial x}+v\frac{\partial v}{\partial y}\right)=-\frac{\partial p}{\partial y}+\mu\left(\frac{\partial^2 v}{\partial x^2}+\frac{\partial^2 v}{\partial y^2}\right) \\ +\rho g\beta(T-T_o) \tag{3}$$

$$\rho c\left(u\frac{\partial T}{\partial x}+v\frac{\partial T}{\partial y}\right)=k\left(\frac{\partial^2 T}{\partial x^2}+\frac{\partial^2 T}{\partial y^2}\right)-S \tag{4}$$

where u, v, p, T, T_o are x-, y- direction velocity, pressure, temperature, and the reference temperature for a fluid property. ρ, c, k, μ, β are density, specific heat, thermal conductivity, viscosity, and volumetric thermal expansion coefficient. By using DOM(Fiveland, 1984) or DS_N (Byun and Smith, 1997a, 1998, 2001), the source function S can be expressed as ;

$$S=4\kappa\sigma T^4-\int_{4\pi}Id\omega=4\kappa\pi I_b-\sum_{k=1}^{4M_o}c_k\omega_k I_k^- \tag{5}$$

The discrete ordinates directions are denoted as c_k, and ω_k is the weighting factor for the k-discrete-ordinates direction, κ is the absorption

coefficient, and M_o is the number of angular directions per quadrant.

The governing equations are discretized in the control volume using SIMPLE methods (Patankar, 1980 ; Myung, 2000). The control volumes are generated by dividing the length, width by n. Subscripts N, S, E, W are assigned for the north, south, east, and west surfaces. The radiative transfer equation (Siegel and Howell, 1993) is discretized to find the intensities by the direct discrete-ordinates methods (DS_N). If the governing equations and boundary conditions are arranged in dimensionless form (Tan and Howell, 1991), the dimensionless variables are Ra, Pr, N, τ, ϵ.

2.2 Boundary conditions and wall heat fluxes

No slip conditions are used for the velocity at the walls. Constant wall temperatures, and constant wall emissivity conditions are specified at the walls as :

@ $x=0$, $0<y<L$, $u=0$, $v=0$, $T=T_W$, $\epsilon=\epsilon_W$ (6a)
@ $x=L$, $0<y<L$, $u=0$, $v=0$, $T=T_E$, $\epsilon=\epsilon_E$ (6b)
@ $y=0$, $0<x<L$, $u=0$, $v=0$, $T=T_S$, $\epsilon=\epsilon_S$ (6c)
@ $y=L$, $0<x<L$, $u=0$, $v=0$, $T=T_N$, $\epsilon=\epsilon_N$ (6d)

The intensity I leaving a gray diffusely emitting and reflecting wall along the k- discrete-ordinates direction is

$$I_{k,w}^+=\frac{1}{\pi}\left[\epsilon_w\sigma T_w^4+\rho_w\sum_{k=1}^{4M_o}c_k\omega_k I_k^-\right] \\ w=N,\ S,\ E,\ W \tag{7}$$

where ϵ_w and ρ_w are wall emissivity and reflectivity, σ is the Stefan-Boltzmann constant, and T_w is the absolute temperature of the wall. The directional cosine is denoted as c_k where $c_k=\mu_k$ for the N, S wall, $c_k=\xi_k$ for the E, W wall. The procedures for computing the values of c_k and ω_k are described in Sanchez and Smith (1992) and also in Byun and Smith (1997a, 2001). The intensity leaving and arriving at the control volume are denoted by the superscript + and −, respectively.

The intensity leaving a gray diffusely emitting but specularly reflecting wall along the k-discrete-ordinates direction is

$$I_{k,w}^{+} = \varepsilon_w I_{bk,w} + \rho_w I_{k,w}^{-}$$
$$w = N, S, E, W \tag{8}$$

where $I_{bk,w}$ is the wall blackbody intensity.

The wall heat flux at each boundary surface, q_w, is assumed to be the same as the sum of the conductive and radiative heat flux leaving the surface.

$$q_w = -k \frac{\partial T}{\partial y}\Big|_w + \sum_{k=1}^{4M_o} c_k \omega_k (I_k^{+} - I_k^{-})$$
$$w = E, W, N, S \tag{9}$$

Weights and directions by Sanchez and Smith's (1992) are used for this study. The procedures for obtaining numerical solutions are the same as used for the standard DOM procedure (Fiveland, 1984). For specular reflection, a special care is taken to follow the computation order. There are four quadrants to scan through for the computation. The computation order between quadrants is specified for this research if there is a specularly reflecting wall. If the kth-directions in the quadrant is such that incident on the specularly reflecting wall, then the next quadrant is chosen such that contains the directions that leaving the specularly reflecting wall after finishing the previous quadrant scanning procedure. If negative intensities occur during the computation then the intensity fix-up process is used by setting these as zero (Byun and Smith, 1998).

3. Results and Discussion

The following accuracy check has been performed. At $\tau = 0$, the view factors are obtained using the current code. For absorbing and emitting medium, DEA and TEA are computed by the current code. These results match well with the previous results by Byun and Smith (1997a, 1998). The results satisfy the symmetry, reciprocity, and enclosure relations. Not only pure conduction but also combined conduction and radiation results agree well with the results by Byun and Han (2001). The results without radiation are verified by Myung (2000). Compaq SMP system with f90 FORTRAN compiler was used for numerical calculations. The number of the spatial divisions n used for the results is 100. The

number of the directions per quardrant M_o used is 128.

In Figs. 2(a) and 2(b), the stream lines and temperature contours are presented under the following conditions. The medium of optical thickness $\tau = 1$ is enclosed by four opaque and black walls. The length of the wall is denoted by L and is 0.1 m. The Rayleigh number specified are $Ra = 0.92 \times 10^6$, $Ra = 0.18 \times 10^6$, for Figs. 2(a) and 2(b), respectively. The south wall temperature is $T_S = 310$ K and $T_S = 302$ K for Figs. 2(a) and 2(b), respectively. All the other walls are at the same low temperature of $T = 300$ K. The fluid properties are evaluated at $T_o = 300$ K and $Pr = 0.71$, but the parameter N is calculated at $T_r = T_S$. The stream lines are presented with a step of 0.0003. Relatively strong fluid circulation is observed at the higher Ra. Thus, the same dimensionless temperature contours move farther toward the cold walls at the higher Ra.

In Fig. 3, dimensionless temperature profiles along the $x/L = 0.5$ lines are presented at different optical thicknesses. Temperatures specified are $T_S = 310$ K and $T_N = T_E = T_W = 300$ K. The fluid properties are evaluated at $T_o = 300$ K and $Pr = 0.71$. All the walls except the north wall are black in this case. The north wall emits diffusely but reflects either diffusely or specularly.

(a) $Ra = 0.92 \times 10^6$, $Pr = 0.71$, $N = 0.039$, $\tau = 1.0$, $\Delta\psi = 0.0003$, $\Delta T = 1$ K

(b) $Ra = 0.18 \times 10^6$, $Pr = 0.71$, $N = 0.042$, $\tau = 1.0$, $\Delta\psi = 0.0002$, $\Delta T = 0.5$ K
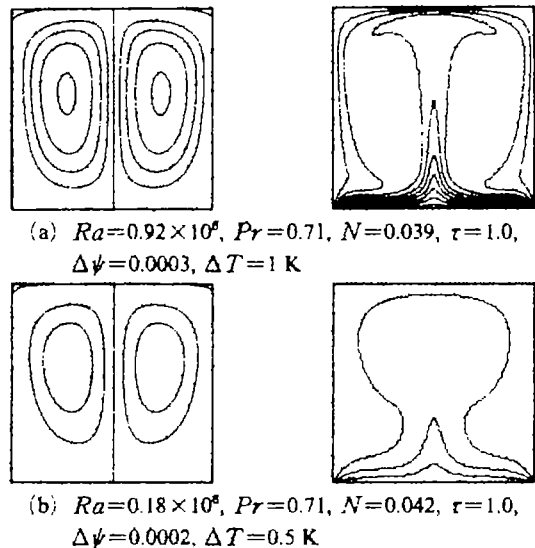
Fig. 2 Stream function and temperature contours

The upper groups are the results for the combined radiation and laminar free convection case at $Ra=0.92\times10^6$. The conduction to radiation parameter for this case is $N=0.039$ that is evaluated at the reference temperature, $T_r=310$ K. The lower groups are for the combined conduction and radiation case. The lower groups are shifted downward by 0.02, and the scale appear on the righthand y-axis.

Without the fluid motion, as the optical thickness increases from 0.1 to 1, the gas temperature profiles for the inner region flattens. The slope of the gas temperature becomes steeper at the hot south wall and declines at the cold north wall. As the optical thickness is increased further, the temperature profile approaches to pure conduction profile. This tendency can be observed by comparing the result for $\tau=0.1$ with $\tau=10$ in Fig. 3. Thus, as the optical thickness increases from 0.1 to 10, the tendency changes around at $\tau=1$.

With the fluid motion, the temperature gradient near the hot and cold wall becomes steep. It is steeper especially near the cold wall than at th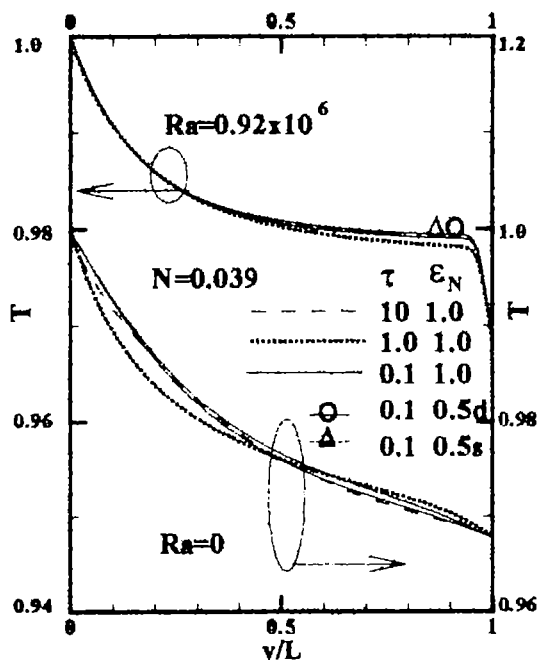e hot wall. The temperature profile for the inner region is rather flattened. At $\tau=0.1$, the effects of the north wall reflection mode on the gas temperature profiles are presented at $\varepsilon_N=0.5$. All the other walls are black. Whether the north wall reflects diffusely or specularly, the middle gas temperature level is higher than the black wall case due to the north wall reflection. Thus, the gas temperature slope at the hot wall decreases. Not much difference in temperature profile along the center line is observed whether the reflection mode is diffuse or specular. It is observed nearly the same stream lines and temperature contour plots for diffuse or specular case. Thus, the results are not presented.

In Fig. 4, dimensionless north wall heat flux results are presented, where $Q=q_w/(\sigma T_r^4)$. The conditions specified are the same as those used for the convection and radiation results in Fig. 3. For each set, upper results are for the total wall heat flux that is the sum of the conductive and the radiative heat fluxes. The lower results are for the wall radiative flux. The results in Fig. 4 indicate that the central region receives more total heat flux than the region near the side wall and the variation of radiative heat flux along the north wall is small. Thus, the conductive flux is larger near the central region and it is because of the fluid motion. As optical thickness increases from
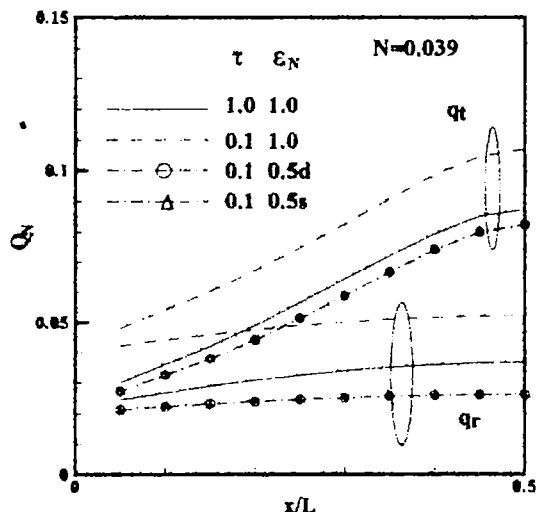

Fig. 3   Dimensionless temperature profiles along the center of the x-axis ($Pr=0.71$, $N=0.039$)

Fig. 4   Dimensionless north wall heat flux ($Ra=0.92\times10^6$, $Pr=0.71$, $N=0.039$)

$\tau=0.1$ to 1, both total and radiative fluxes decrease at the north wall. The total and radiative flux results for the specularly reflecting wall should be the same as those for the diffusely reflecting wall as can be confirmed in Fig. 4.

In Fig. 5, the dimensionless east wall heat flux distribution is presented. Due to symmetry, it is the same as the west wall. The specular or diffuse reflections occurs at the north wall. Temperatures specified are $T_S=310$ K and $T_N=T_E=T_W=300$ K. The fluid properties are evaluated at $T_o=300$ K and the reference temperature T_r is 310 K. Also, $Ra=0.92\times10^6$, $Pr=0.71$, and $N=0.039$. North wall emissivity is $\varepsilon_N=0.5$. The results presented are at $\tau=0.1$ and $\tau=1.0$. Both total and radiative fluxes are less at $\tau=1$ than at $\tau=0.1$ because transmission decreases with increasing optical thickness. Only the results for diffuse reflection case are presented at $\tau=1$ because the results between two reflection modes do not show much difference at τ greater than 1. Both total and radiative fluxes on the east wall are less with specularly reflecting north wall than with diffusely reflecting north wall due to the geometry of the problem. The difference between two reflection modes is larger near the cold north wall where $y/L=1$. The difference diminishes
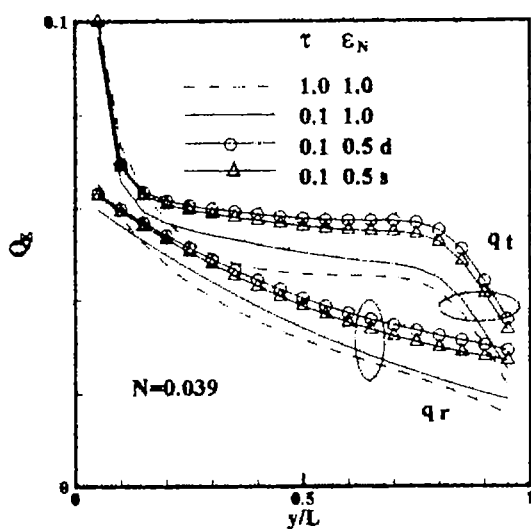
as approaching the hot south wall where $y/L=0$.

In Fig. 6, the stream function and temperature contour plots at the two different reflection modes are presented under the following condition. Temperatures specified are $T_S=827$ K, $T_N=T_E=T_W=600$ K, and $T_r=827$ K. The air properties at $T_o=600$ K are used for the fluid property. Thus, $Pr=0.68$ and $Ra=0.92\times10^6$, and are about the same as for Figs. 3-5 results. However N is reduced about one order of magnitude as $N=0.0037$. Absorption coefficient is $\kappa=1$ m^{-1}, $L=0.1$ m, and thus $\tau=0.1$. Except $\varepsilon_N=0.5$ at the north wall, all the other walls are opaque and black. The north wall emits diffusely but reflects diffusely or specularly. The contour levels for the stream function are 0.001. The temperature contour levels are 625, 650, 675, 680, 685, 690, 695, 700, 725, and 800 K. Not much difference in flow characteristics is observed, even though there is a slight lift in the streamlines for specular reflection case. Except near the central regions, not much difference in the gas temperature profiles is observed. The temperature contours for specular reflection advance more to the north wall and less to the sides near the hot south wall (680 K). It is because specular reflections send more energy back to the hot south wall than the diffuse reflections for this geometry. On the other hand, the reversal of the tendency can be noted near the cold north wall (685 K). Due to symmetry, west wall shows the same tendencies as the east wall. If the north wall is black with $\tau=1$, the computation is divergent or result in unsymmetric
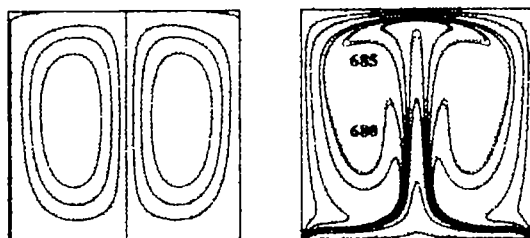

Fig. 5 Effects of reflection mode on dimensionless east wall heat flux ($Ra=0.92\times10^6$, $Pr=0.71$, $N=0.039$, $\tau=0.1$)

Fig. 6 Stream function and temperature contours for diffuse (solid line) or specular (dotted line) north wall ($Ra=0.92\times10^6$, $Pr=0.68$, $N=0.0037$, $\tau=0.1$, $\varepsilon_N=0.5$, $\Delta\psi=0.001$, $T=625$, 650, 675, 680, 685, 690, 695, 700, 725, 800 K)

contours unless Ra less than about 3×10^5. Thus, the reflection by the north wall may stabilize the flow field and delay the transition to the turbulent flow if it is not a numerical error. For the results obtained with $\tau=1$ at other Ra, the difference caused by the reflection mode influences more to the contour plots than with $r=0.1$. Fig. 6 is one of the typical plots showing the difference.

In Fig. 7, the dimensionless east wall heat flux distribution along the y-axis is presented for specularly and diffusely reflecting north wall. Conditions specified are the same as those for Fig. 6. Total (with symbol) and radiative (without symbol) wall heat fluxes are presented. Radiative fluxes are always less than the total heat fluxes. Wall heat fluxes with specular reflection are always less than those with diffuse reflection. The difference is larger near the north wall and it decreases near the cold wall. The slope of the wall heat fluxes is greater for the specular case than for the diffuse case. For comparison purpose, the heat flux results for $\tau=0.01$ with diffusely reflecting wall case are presented. Total heat flux is about the same as with $\tau=0.1$ case, however the radiative flux is larger for $\tau=0.01$ due to decreased attenuation by the medium. At $\tau=0.1$, the maximum deviations relative to the diffuse reflection

results are 8.7, 8.2% for total and radiative flux, separately. At $\tau=0.1$, the deviations are increased to 9.1, 9.7%. The differences in the total heat fluxes are about the same as those in the radiative heat fluxes. At $\tau=1.0$, the differences in the wall heat flux between the two reflection modes almost disappear. Thus the results are not drawn in Fig. 7. Though differences are small at $\tau=1.0$, the diffuse reflection case has slightly higher values than the specular cases. As optical thickness increases from 0.01 to 1, the total and radiative fluxes near the cold wall decrease. But they increase near the hot south wall. Therefore, the flux variation along the y-axis increases.

In Fig. 8, the effects of the north wall emissivity on total wall heat flux distribution along the east wall are presented for specular and diffuse north wall case. Two sets of total heat flux results at $Ra=0.92 \times 10^6$ and $Ra=1 \times 10^5$ are presented by varying the north wall emissivity to 0.8, 0.5, and
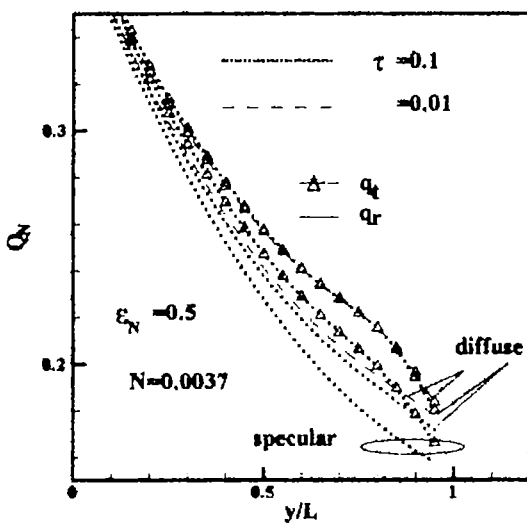
Fig. 7 Effects of reflection mode on dimensionless east wall heat flux $(Ra=0.92 \times 10^6,\ Pr=0.68,\ N=0.0037,\ \varepsilon_N=0.5)$
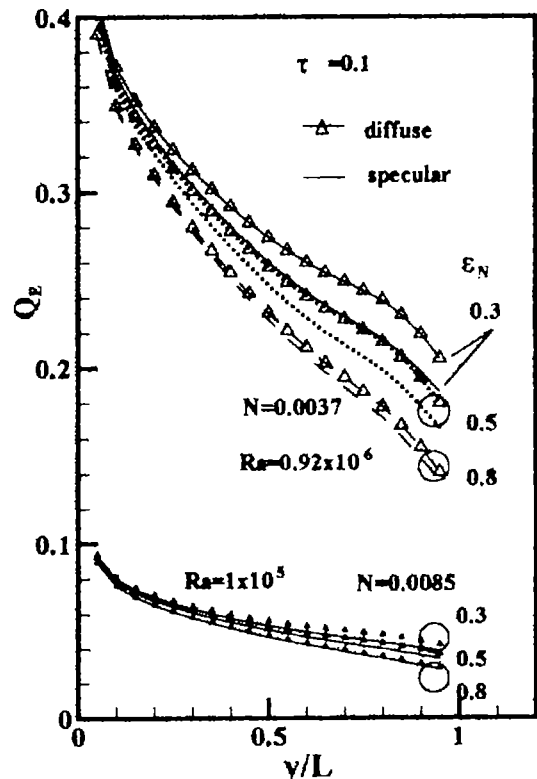
Fig. 8 Effects of emissivity on dimensionless total east wall heat flux $(Pr=0.68,\ \tau=0.1)$

0.3. For the upper set of Ra, the conditions specified are the same as those used for the Figs. 6-7 except for the north wall emissivity. The only difference in the conditions specified for upper and lower set is the south wall temperature; $T_S = T_r = 827$ K for $Ra = 0.92 \times 10^6$, and $T_S = T_r = 625$ K for $Ra = 1 \times 10^5$ while $T_N = T_E = T_w = 600$ K. The optical thickness is 0.1, and $Pr = 0.68$. The results with symbol represent the diffuse case and the lines are used for the specular case. As before, total wall heat flux for diffuse north wall is always larger than that for specular north wall. As the north wall emissivity decreases, the total heat fluxes on the east wall increase mostly due to the increase in the radiative heat flux. The increase near the cold north wall is larger. Near the south wall, the increase is lowered. As the wall emissivity decreases, the gap between two reflection modes increases except near the hot south wall. At $Ra = 0.92 \times 10^6$, the

maximum deviations in the total heat flux for diffuse reflection case results are 3.9%, 8.2%, 9.8% at $\varepsilon_N = 0.8$, 0.5, 0.3, respectively. The deviations in the radiative flux are 4.3, 8.7, 10.4%. At $Ra = 10^5$, the deviations in the radiative flux are 4.0, 8.0, 9.9% at $\varepsilon_N = 0.8$, 0.5, 0.3, respectively. The deviations in the radiative flux are 4.3, 8.4, 10.3% in this case. As Ra decreases, the magnitude of total heat flux also decreases. However, the percentage deviations are about the same as before. The trends observed for $Ra = 0.92 \times 10^6$ results are still valid.

In Fig. 9, dimensionless total east wall heat fluxes distribution along the y-axis are presented for specularly and diffusely reflecting north wall. Solid lines, and symbols denotes specularly, and diffusely reflecting case, respectivly. Conditions specified are; $Ra = 1 \times 10^5$, $Pr = 0.68$, $N = 0.0085$, $\varepsilon_N = 0.5$, and $\tau = 0.1$ or $\tau = 1.0$. For comparison purpose, the radiative fluxes for specular reflection are drawn with dotted lines. The same trends as observed in Fig. 7 are shown.

4. Conclusions

The effect of specularly reflecting wall on the combined radiative and laminar free convective heat transfer in an infinite square duct are studied by using the direct discrete ordinates method. The medium is absorbing and emitting with gray properties. One of the wall emits diffusely but reflects diffusely or specularly.

For the range of Ra studied, N is an important parameter that tells whether the differences can be observed in the streamlines, the temperature profiles, and the wall heat flux. The differences are indistinguishable unless radiation is a dominant mode of heat transfer such that N is about the order of 10^{-3} or less.

If radiation is a dominant mode, the optical thickness is a parameter that predicts if some differences are observed in the wall heat fluxes on the wall receiving the reflected energy. For optically thin systems, the differences caused by different reflection mode are observed. The difference is decreased with increasing optical thickness. As N decreases, the differences are observed
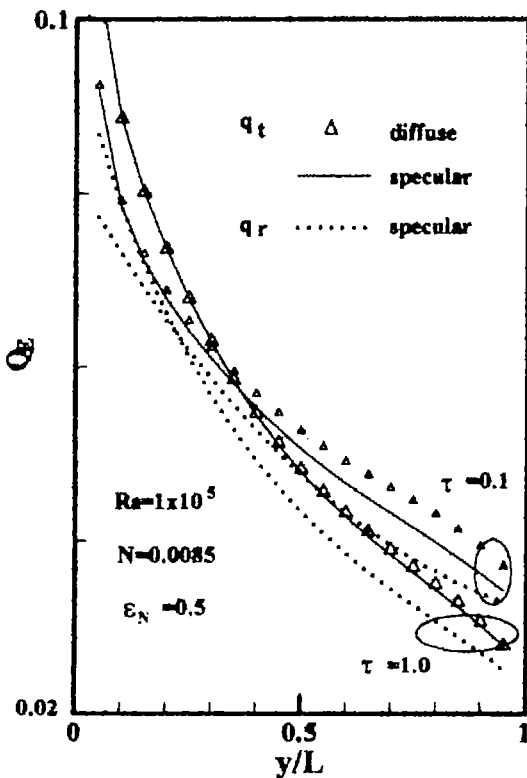

Fig. 9 Effects of optical thickness on dimensionless east wall heat flux ($Ra = 10^5$, $Pr = 0.68$, $N = 0.0085$, $\varepsilon_N = 0.5$)

at higher optical thickness. As the wall emissivity decreases, the differences between these two modes of reflections increase. The side wall heat fluxes with diffuse reflection are always higher than those with specular reflection.

As long as radiation dominates heat transfer, the difference still can be observed in the streamlines or the temperature contours, but it is not as distinctive as in the wall heat flux distributions. It needs further study.

Acknowledgment

References

Bae, K., Chung, H. and Jeong, H., 2002, "Convective Heat Transfer in Ventilated Space with Various Partitions," *KSME Int. J.*, Vol. 16, No. 5, pp. 676~682.

Byun, K. H., Smith, T. F. and Sanchez, A., 1997a, "View Factors of a Rectangular System Enclosing Transparent Media by Discrete-ordinates Method," *KSME Int. J.*, Vol. 11, No. 3, pp. 331~338.

Byun, K. H. and Smith, T. F., 1997b, "View Factors for Rectangular Box Type Enclosures by the Direct Discrete-Ordinates Method," *J. of Thermophysics and Heat Transfer*, Vol. 11, No. 4, pp. 593~595.

Byun, K. H. and Smith, T. F., 1998, "Total Exchange Areas for Rectangular Enclosures with Reflecting Wall by the Direct Discrete-Ordinates Method," *Proc. of 11th IHTC*, Vol. 3, pp. 319~324, Kyongju, Korea.

Byun, K. H. and Han, D. C., 2001, "Effects of Speculary Reflecting Wall in an Infinite Square Duct on Conductive-Radiative Heat Transfer," *Transactions of the KSME*, Vol. B25, No. 10, pp. 1451~1458(in Korean).

Cai, W., 1998, "Radiative Heat Transfer Model in Arbitrary Enclosures by Ray-tracing," Radia-

tive Transfer-II, Begell House, Inc., New York.

Fiveland, W. A., 1984, "Discrete-Ordinates Solutions of the Radiative Transport Equation for Rectangular Enclosures," *J. of Heat Transfer*, Vol. 106, pp. 699~706.

Fusegi, T. and Farouk, B., 1988, "Numerical and Experimental Study of Natural Convection-Radiation Interactions in a Non-gray Gas filled Square Enclosure," *Proc. of the 1st KSME-JSME Thermal Engineering Conf.*, Vol. 2, pp. 415~420, Seoul, Korea.

Iwatsu, R. and Hyun, J. M., 1996, "Numerical Simulation of Natural Convection with Large Temperature Differences-Steady Solutions at $Pr=0.71$," *Proc. of the 3rd KSME-JSME Thermal Engineering Conf.*, Vol. 1, pp. 59~64, Kyongju, Korea.

Lauriat, G., 1982, "Combined Radiation-Convection in Gray Fluids Enclosed in Vertical Cavities," *J. of Heat Transfer*, Vol. 104, pp. 609~615.

Lee, T. S. and Lee, J. S., 1988, "Numerical Predictions of Three Dimensional Natural Convection in a Box," *Proc. of the 1st KSME-JSME Thermal Engineering Conf.*, Vol. 2, pp. 278~283, Seoul, Korea.

Maruyama, S., 1993, "Radiation Heat Transfer between Arbitrary Three-Dimensional Bodies with Specular and Diffuse Surfaces," *Numerical Heat Transfer*, Part A., Vol. 24, pp. 181~196.

Myung, H. K., 2000, Computer-Aided Engineering for Heat Transfer and Fluid Flow (in Korean), Mun Un Dang Publ. Co., Seoul.

Patankar, S. V., 1980, *Numerical Heat Transfer and Fluid Flow*, McGraw-Hill, New York.

Sanchez, A. and Smith, T. F., 1992, "Surface Radiation Exchange for Two-Dimensional Rectangular Enclosures Using the Discrete-ordinates Method," *J. of Heat Transfer*, Vol. 114, pp. 465~472.

Siegel, R. and Howell, J. R., 1993, *Thermal Radiation Heat Transfer*, Hemisphere Publishing, Washington, DC.

Tan, Z. and Howell, J. R., 1991, "Combined Radiation and Natural Convection in a Two-Dimensional Participating Square Medium," *Int. J. Heat Mass Transfer*, Vol. 34, No. 3, pp. 785~793.